

1 <https://v1.overleaf.com/15790648swrpvqxhkshy>

2 Deep Underground Neutrino Experiment (DUNE)

3 DRAFT Technical Design Report

4 **Volume n/a:**

5 (Calibration Information for SP volumes)

6 March 8, 2019

7 The DUNE Collaboration

Contents

10	Contents	i
11	List of Figures	iii
12	List of Tables	iv
13	1 Calibration Hardware for Single-Phase	1
14	1.1 Calibration Hardware Overview	1
15	1.1.1 Introduction	1
16	1.1.2 Scope	2
17	1.1.3 Requirements	2
18	1.1.4 Design Considerations	3
19	1.1.4.1 Cryostat Configuration for Calibration	3
20	1.2 Laser Calibration Systems	4
21	1.2.1 Ionization Laser System	4
22	1.2.1.1 Physics Motivation	4
23	1.2.1.2 Requirements	5
24	1.2.1.3 Design	6
25	1.2.1.4 Possible Measurements	11
26	1.2.2 Photoelectron Laser System	12
27	1.2.2.1 Physics Motivation	12
28	1.2.2.2 Design	12
29	1.2.2.3 Possible Measurements	13
30	1.2.3 Laser positioning system	13
31	1.2.3.1 Physics Motivation	13
32	1.2.3.2 Design	13
33	1.2.3.3 Possible measurements	14
34	1.3 Pulsed Neutron Source Calibration System	15
35	1.3.1 Physics Motivation	15
36	1.3.2 Design	16
37	1.3.3 Possible Measurements	19
38	1.3.3.1 Capture Cross-Section and Gamma Cascade	19
39	1.3.3.2 Cryostat Materials Activation Measurement	19
40	1.3.3.3 Scattering Cross-Section Measurement	19
41	1.3.3.4 Test Deployment in ProtoDUNE-SP	20
42	1.4 Alternative System: Radioactive Source Calibration System	20

43	1.4.1	Physics Motivation	20
44	1.4.2	Design	20
45	1.4.3	Possible Measurements	21
46	1.5	DAQ Requirements	22
47	1.5.1	Laser Calibration	22
48	1.5.2	Radioactive Sources	23
49	1.5.3	Intrinsic Radioactivity	23
50	1.6	Validation of Calibration Hardware Systems	24
51	1.6.1	Validation in ProtoDUNE	24
52	1.6.2	Validation in Other Experiments	25
53	1.7	Organization and Management	25
54	1.8	Interfaces	26
55	1.9	Cost	26
56	1.10	Risks	27
57	1.11	Quality Control	27
58	1.12	Safety	28
59	1.12.1	Human Safety	28
60	1.12.2	Detector and System Safety	29
61	1.13	Installation, Integration and Commissioning	29
62	1.13.1	ITF integration	30
63	1.13.2	Installation	30
64	1.14	Institutional Responsibilities	31
65	1.15	Schedule and Milestones	32
66		Glossary	33
67		References	35

List of Figures

70 1.1 Top view of the SP detector module cryostat showing various penetrations. Highlighted
71 in black circles are multi-purpose calibration penetrations. The orange dots are TPC
72 signal cable penetrations. The blue ports are detector support system (DSS) penetra-
73 tions. The orange ports are TPC signal cable penetrations. The larger purple ports at
74 the four corners of the cryostat are manholes. 3

75 1.2 Left: Schematics of the ionization laser system in one port (from[1]). Right: Schematics
76 of the laser box (from[2]). 7

77 1.3 Left: CAD drawing of the MicroBooNE feedthrough. Right: CAD drawing of the
78 MicroBooNE periscope. Both figures from[2]. 8

79 1.4 CAD drawing of a possible way for the periscope to penetrate the FC. 9

80 1.5 Signal from the GaP pin diode. The signal was result of illumination of the PIN diode
81 face with 266 nm at room temperature. 14

82 1.6 Signal from the GaP pin diode. The signal was result of illumination of the PIN diode
83 face with 266 nm at cryogenic temperature. 14

84 1.7 LPS cluster that is mounted on the opposite wall from the laser periscope to detect and
85 accurately determine the end point of the laser beam. 14

86 1.8 Profile of the LPS group mounted on the PCB. GaP diodes come with pins that utilize
87 twisted pair to transport the signal. 14

88 1.9 Three designs of the Pulsed Neutron Source 17

89 1.10 Energy of neutrons injected to the liquid argon TPC volume.Simulation based one Design
90 B. 18

91 1.11 Top view of the protoDUNE-SP cryostat showing various penetrations. Ports marked in
92 red are present free and they could be used for tests of the calibration systems. The four
93 largest ones have the same diameter (250 mm) of the calibration ports of DUNE-FD,
94 and are located over the TPC. The two larger ports at the right-hand side corners of
95 the cryostat are the human access ports (or manholes). 24

96 1.12 Organizational chart for the Calibration Consortium. 25

98 **List of Tables**

99 1.1 Calibration System Cost Summary 27
100 1.2 High Voltage System Risk Summary 27
101 1.3 High Voltage System Schedule 31
102 1.4 Calibration System Schedule 32

103

Todo list

105	Discuss development plan on way to building	21
106	Add or reference DAQ summary table that has been prepared	22
107	Add estimate of laser positioning system, DAQ/computers, racks? cables?	26
108	sample from HV - use as template	27
109	This is a copy of text we sent to Jim Stewart for the integration chapter.	27
110	We also want to reference common installation and commissioning safety concerns– like work at	
111	heights, falling object risk, overhead crane operation, heavy objects, electrical safety etc. Is	
112	there a common document/section we can reference for this?	28
113	This may be a shared concern. We want to avoid bumping/breaking components as they are	
114	checked, installed and commissioned in DUNE. Special care will need to be taken to install	
115	components and do checks stepwise.	29
116	Jose, mitigation is?	29
117	relationship between this and interface with PD?	29
118	May also need to reference background TF. Add RS system.	29
119	We have started discussions about electrical safety and grounding, and will update this once	
120	formal documents are prepared for that.	29
121	This is a copy of text we sent to Jim Stewart for the integration chapter. We need guidance for	
122	how this chapter and that chapter need to reference each other.	29
123	Need to confirm this with groups, esp CSU, Pitt doing general simulation work and understand	
124	what further subdivision is useful. We are also seeking new groups.	31
125	The laser system schedule will look similar to the pulsed neutron source– but we need to confirm	
126	the TCO closing/installation period before filling in a table for it.	32
127	Mar 2023	32
128	Jun 2023	32

Chapter 1

Calibration Hardware for Single-Phase

1.1 Calibration Hardware Overview

1.1.1 Introduction

A detailed understanding of the overall detector response is essential for DUNE physics goal. The precision with which each calibration parameter needs to be measured is set by the systematic uncertainties for the long-baseline (LBL) and other physics programs at DUNE. Chapter 4 of the Physics volume of the TDR provides a detailed description of the calibration strategy for DUNE using existing sources of particles (e.g. cosmic ray muons), external measurements (e.g. ProtoDUNE), monitors (e.g. purity monitors) and dedicated calibration hardware systems.

Chapters 3, 4, 5 and 8 describe other hardware that are essential for calibration such as cold electronics (CE) external charge injection systems, high voltage (HV) monitoring devices, photon detection system (PDS) stability monitoring system, and cryogenic instrumentation and detector monitoring devices, respectively. The usage of existing sources of particles, and external measurements is discussed in the physics volume of the TDR. This chapter describes the dedicated calibration systems, to be deployed for the DUNE SP detector module which are intended to provide information beyond the reach of the other calibration sources. These include an ionization laser system, a photoelectron laser system and a pulsed neutron source system. The possibility of deploying a radioactive source system is also currently being explored.

Section 1.1.2 describes the baseline hardware designs, and outlines alternative designs which may improve physics capability and/or reduce overall cost. Section 1.2 describes the baseline design for the ionization laser system, used to map out the electric field throughout the detector. Section ?? describes the baseline design for the pulsed neutron source, which can be used to provide a known deposit of energy across the entire detector volume.

The Calibration Consortium was formed in November 2018. As such, significant development plans

154 exist and the timeline for these is outlined in Section 1.15.

155 **1.1.2 Scope**

156 **1.1.3 Requirements**

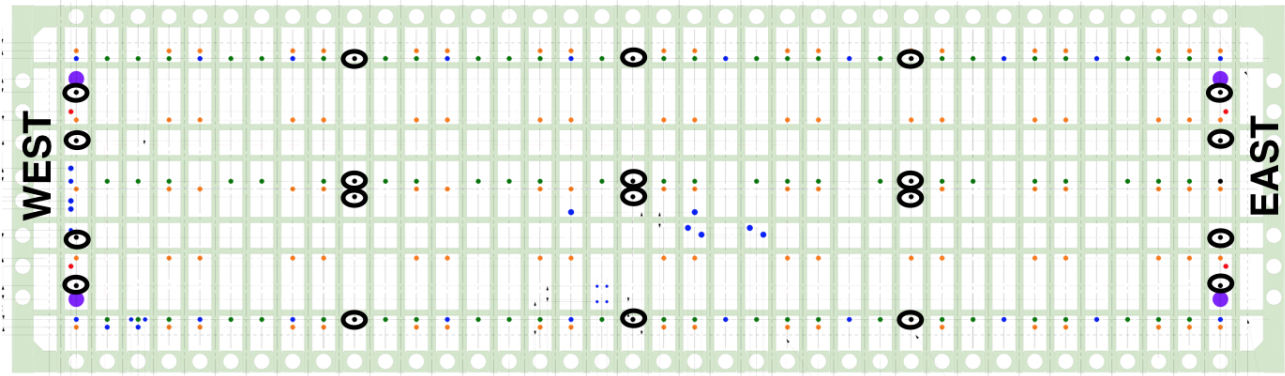


Figure 1.1: Top view of the SP detector module cryostat showing various penetrations. Highlighted in black circles are multi-purpose calibration penetrations. The orange dots are TPC signal cable penetrations. The blue ports are DSS penetrations. The orange ports are TPC signal cable penetrations. The larger purple ports at the four corners of the cryostat are manholes.

157 1.1.4 Design Considerations

158 1.1.4.1 Cryostat Configuration for Calibration

159 The current cryostat design for the SP detector module with penetrations for various sub-systems
 160 is shown in Figure 1.1. The penetrations dedicated for calibrations are highlighted in black circles.
 161 The ports on far east and far west are located outside the field cage. The current plan is to
 162 use these penetrations for multiple purposes. For example, the penetrations on the far east and
 163 west will be used both by laser and radioactive source deployment systems. In addition to these
 164 dedicated ports, the Detector Support System (DSS) and cryogenic ports (orange and blue dots
 165 in Figure 1.1, respectively) will also be used as needed to route cables for the single phase photon
 166 detector calibration system. The DSS and cryogenic ports are accommodated with feedthroughs
 167 with a CF63 side flange for this purpose.

168 The placement of these penetrations was driven by the ionization track laser and radioactive source
 169 system requirements. The ports that are closer to the center of the cryostat are placed near the
 170 APAs (similarly to what is planned for SBND) to minimize any risks due to the HV discharge. For
 171 the far east and west ports, HV is not an issue as they are located outside the field cage (FC) and the
 172 penetrations are located near mid-drift to meet radioactive source requirements. Implementation
 173 of the ionization track laser system proposed in Section 1.2.1, requires 20 feedthroughs to cover the
 174 four TPC drift volumes; this arrangement is needed for lasers to be used for full volume calibration
 175 of the electric field and associated diagnostics (e.g. HV).

176 The distance between any two consecutive feedthrough columns in Figure 1.1 is assumed to be
 177 about 15 m. This is considered reasonable since the experience from the MicroBooNE laser system
 178 has shown that tracks will propagate over that detector's full 10 m length. Assuming that the
 179 effects of Rayleigh scattering and self-focusing (Kerr effect) do not limit the laser track length, this
 180 laser arrangement could illuminate the full volume with crossing track data. It is important to
 181 note that at this point in time, a maximum usable track length is unknown and it is not excluded

182 that the full 60 m detector module length could be achieved by the laser system after optimization.

183 1.2 Laser Calibration Systems

184 1.2.1 Ionization Laser System

185 1.2.1.1 Physics Motivation

186 The primary purpose of a laser system is to provide an independent, fine-grained estimate of the
187 E field in space and time. Through its effect on drift velocity and recombination, the E field is
188 a critical parameter for physics signals as it ultimately impacts the spatial resolution and energy
189 response of the detector.

190 There are multiple sources which may distort the electric field temporally or spatially in the
191 detector. Current simulation studies indicate that positive ion accumulation and drift (space
192 charge) due to ionization sources such as cosmic rays or ^{39}Ar is small in the DUNE far detector
193 (FD); however, not enough is known yet about the fluid flow pattern in the FD to exclude the
194 possibility of stable eddies which may amplify the effect for both SP and DP modules. This
195 effect can get further amplified significantly in the DP module due to ion accumulation at the
196 liquid-gas interface. Additionally, other sources in the detector (especially detector imperfections)
197 can cause E field distortions. For example, field cage resistor failures, non-uniform resistivity in
198 the voltage dividers, CPA misalignment, CPA structural deformations, and APA and CPA offsets
199 and deviations from flatness can create localized E field distortions. In both SP and DP systems,
200 the failure of a resistor will create significant, local electric field distortions which will need to
201 be identified¹. While the resistor failure will be detected temporally, its location in space is not
202 possible to determine from monitoring data. Misalignments of detector objects or deformations
203 may also create (small) electric field distortions; while individual effects may be small, it is possible
204 to have a combined, significant effect. Each individual E field distortion may add in quadrature
205 with other effects, and can reach 4% under certain conditions. Understanding all these effects
206 require in-situ measurement of E field for proper calibration.

207 Many useful secondary uses of laser include alignment (especially modes that are weakly con-
208 strained by cosmic rays), stability monitoring, and diagnosing detector failures (e.g., HV). Mis-
209 alignment may include physical deformation and/or rotations of objects within the detector. Cer-
210 tain alignment “directions” difficult to assess with cosmic rays alone, such as distortions of the
211 detector that preserve the gap widths and do not shift the anode plane assemblies (APAs) in x near
212 the gaps relative to one another are difficult to assess with cosmic rays alone. These distortions
213 include global shifts and rotations in the locations of all detector elements, and crumpling modes
214 where the edges of the anode plane assemblies hold together but angles are slightly different from
215 nominal.

¹In the DP system, four registers would have to fail to cause a failure across the field cage gap, but even one failure in the SP can have an impact; this may be partially mitigated by modifying the HV, but not completely.

216 A laser system also has the intrinsic advantage of being immune to recombination, thus eliminating
 217 particle-dependent effects.

218 1.2.1.2 Requirements

219 The energy and position reconstruction requirements for physics measurements lead to require-
 220 ments on the necessary precision of the calibration E field measurement and its spatial granularity.

221 As mentioned in the DUNE Physics TDR (Section 4.4.1.1), a 1% bias in the lepton energy scale
 222 is significant for the LBL sensitivity to CPV. Since a smaller E field leads to higher electron/ion
 223 recombination and therefore a lower collected charge, distortions of the E field are one of the
 224 possible causes of an energy scale bias. According to [4], a 1% distortion on E field leads to a 0.3%
 225 bias on collected charge. Since other effects will contribute to the lepton energy scale uncertainty
 226 budget, we consider a goal for the calibration system to measure the E field to a precision of $\sim 1\%$
 227 so that its impact on the collected charge is well below 1%.

228 The IDR states that a fiducial volume uncertainty of 1% is required (ref. [5], p. 4-46) and that
 229 this translates to a position uncertainty of 1.5 cm in each coordinate (ref. [6], p. 2-12). Also that
 230 in the y and z coordinates, the wire pitch of 4.7 mm achieves that while in the drift (x) direction,
 231 the position is calculated from timing so it is claimed it should be known better.

232 But the position uncertainty depends also on the electric field, via the drift velocity. Since the
 233 position distortions accumulate over the drift path of the electron, it is not enough to specify an
 234 uncertainty on the field, we must accompany it by specifying the size of the spatial region of that
 235 distortion. i.e. a 10% distortion would not be relevant if it was confined to a 2 cm region, for
 236 instance, and the rest of the drift region was nominal. So what matters is the product of [size of
 237 region] \times [distortion]. Moreover, we should distinguish distortions of two types:

- 238 1. affecting the magnitude of the field. Then the effect on the drift velocity v is also a change
 239 of magnitude. According to the function provided in [7], close to 500 V/cm, the variation of
 240 the velocity with the field is such that a 4 % variation in E leads to a 1.5 % variation in v .
- 241 2. affecting the direction of the field. Nominally, the field E should be along x , so $E = E_L$
 242 (the longitudinal component). If we consider that the distortions introduce a new transverse
 243 component E_T , in this case this translates directly into the same effect in the drift velocity,
 244 that gains a v_T component that is $v_T = v_L E_T / E_L$, i.e. a 4 % transverse distortion on the field
 245 leads to a 4 % transverse distortion on the drift velocity.

246 So, a 1.5 cm shift comes about from a constant 1.5 % distortion in the velocity field over a region
 247 of 1 m. In terms of electric field, that could be from a 1.5 % distortion in ET over 1 m or a 4 %
 248 distortion in EL over the same distance.

249 From ref. [5], page 4-53, E field distortions can be caused by space-charge effects due to accumula-
 250 tion of positive ions caused by ^{39}Ar decays (cosmic rate is low in FD), or detector defects, such as
 251 field cage resistor failures, resistivity disuniformities, etc... The total effects added in quadrature

252 can be as high as 4 %. From ref. [4], the space charge effects due to ^{39}Ar can be of the order of 0.1 %
253 for the single phase (SP), and 1 % for the dual phase (DP), so in practice that kind of distortion
254 needs to cover several meters in order to be relevant. Other effects due to cathode plane assembly
255 (CPA) or field cage (FC) imperfections can be higher than those due to space charge, but they
256 are also much more localized. If we assume that there are no foreseeable effects that would distort
257 the field more than 4 %, and considering the worst case (transverse distortions), then the smallest
258 region that would produce a 1.5 cm shift is $1.5/0.04 = 37.5$ cm. That provides a target for the
259 granularity of the measurement of the E field distortions in x , with of course a larger region if the
260 distortions are smaller. Given the above considerations, then a voxel size of $10 \times 10 \times 10$ cm appears
261 to be enough to measure the E field with the granularity needed for a good position reconstruction
262 precision. In fact, since the effects that can likely cause bigger E field distortions are the problems
263 or alignments in the CPA (or APA), or in the FC, it could be conceivable to have different size
264 voxels for different regions, saving the highest granularity of the probing for the walls/edges of the
265 drift volume.

266 1.2.1.3 Design

267 1.2.1.3.1 Baseline design

268 The design of the laser calibration system for DUNE is strongly based on the design of the system
269 built for MicroBooNE [2], that was based on several previous developments[8, 9, 10, 11]. A similar
270 system was also built for CAPTAIN[12] and SBND[1]. Operation of the MicroBooNE system has
271 already taken place and a preliminary report was given in[13].

272 Ionization of liquid argon (LAr) by laser can occur via a multiphoton process in which a two-
273 photon absorption[14] leads the atom to the excited states band, and a third photon can cause
274 ionization. This can only occur with high photon fluxes, and so the employed lasers need to be
275 pulsed and have pulse energies of 60 mJ or more. Contrary to muons, the laser beams do not
276 suffer multiple scattering and travel along straight lines determined by the steering mirror optics.
277 The basic measurement consists in recording the laser beams with the TPC and comparing the
278 reconstructed tracks with the direction known from the steering hardware. An apparent curvature
279 of the measured track is attributed to E field distortions (either in direction or magnitude).

280 An unambiguous field map requires crossing laser tracks in every relevant "voxel" of the detector.
281 If two tracks that enter the same spatial voxel ($10 \times 10 \times 10 \text{cm}^3$ volume) in the detector module,
282 the relative position of the tracks provides an estimate of the local 3D E field.

283 With a single, steerable laser track, there would be ambiguity in the direction/magnitude of the
284 position displacement and so the information obtained would be limited. Even if not crossing, a set
285 of several tracks from opposite directions can still be used to obtain a displacement map via an
286 iterative procedure[13].

287 Laser beams with lengths of 10 m in LAr have been observed in MicroBooNE, and beams with 20 m
288 (possibly more) are reasonably expected to be possible to obtain with a similar system. While the

289 Rayleigh scattering of the laser light is about 40 m, additional optics effects, including self-focusing
 290 (Kerr) effects may limit the maximum practical range. This has determined the choice of locating
 291 5 calibration ports in the cryostat roof at 15 m intervals along each of the 4 drift volumes of the
 292 SP module, for a total of 20 ports. In fact, there are 4 ports just outside each of the FC end-walls,
 293 and 12 ports located over the top FC, close to the APA of each drift volume, as shown in Fig. 1.1.

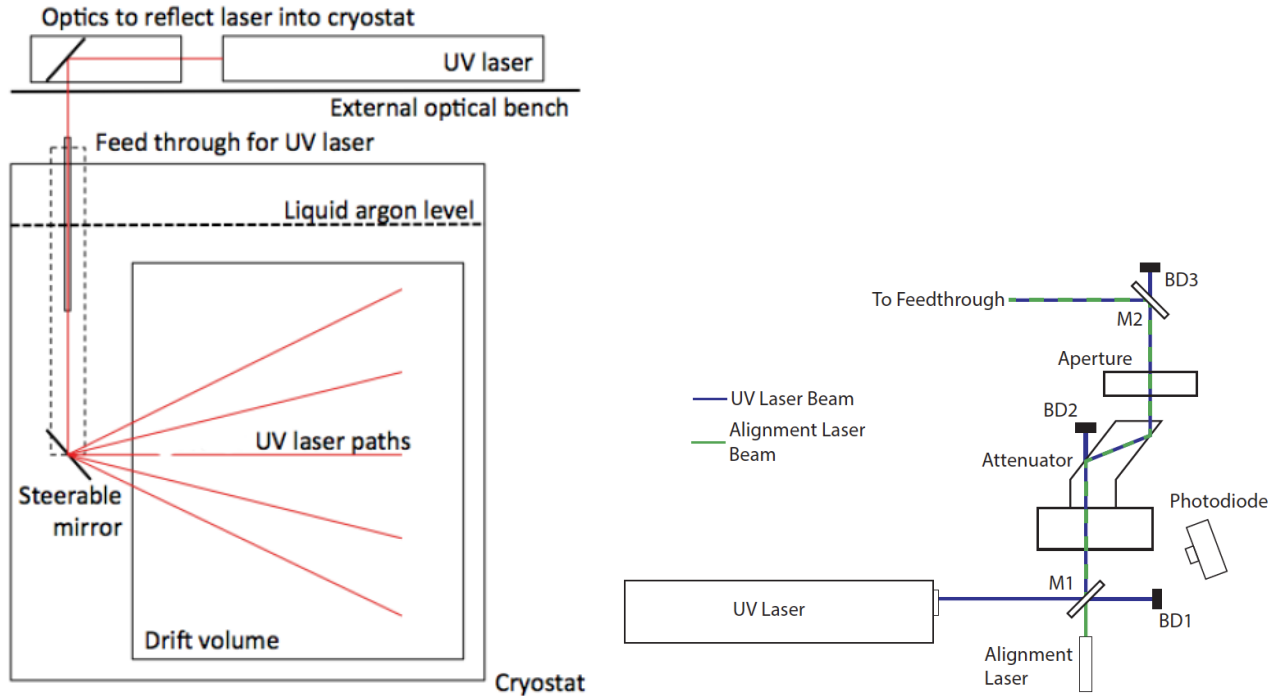


Figure 1.2: Left: Schematics of the ionization laser system in one port (from[1]). Right: Schematics of the laser box (from[2]).

294 For each of those 20 ports, a laser module can be schematically represented by Fig. 1.2 (Left), and
 295 consists of the following elements:

- 296 • a laser box Fig. 1.2 (Right) that provides:
 - 297 – an attenuator and a collimator to control the intensity and size of the beam;
 - 298 – a photodiode that gives a TPC-independent trigger signal;
 - 299 – a low-power red laser, aligned with the UV one, to facilitate alignment operations;
 - 300 – a Faraday cage to shield the surrounding electronics from the accompanying EM pulse.
- 301 • a feedthrough (Fig. 1.3 (Left)) into the cryostat that provides:
 - 302 – and optical coupling that allows the UV light to pass through into the cryostat directly
 - 303 into the liquid phase, avoiding distortions due to the gas-liquid interface and the gas
 - 304 itself;

- 305 – a rotational coupling that allows the whole structure to rotate while maintaing the
- 306 cryostat seal;

- 307 – a periscope structure (Fig. 1.3 (Right)) mounted under that rotating coupling, that
- 308 supports a mirror within the LAr;

- 309 – the additional theta rotation of the mirror is accomplished by a precision mechanism
- 310 coupled to an external linear actuator;

- 311 – both the rotation and linear movements of the steering mechanism are read-out by
- 312 precision encoders.

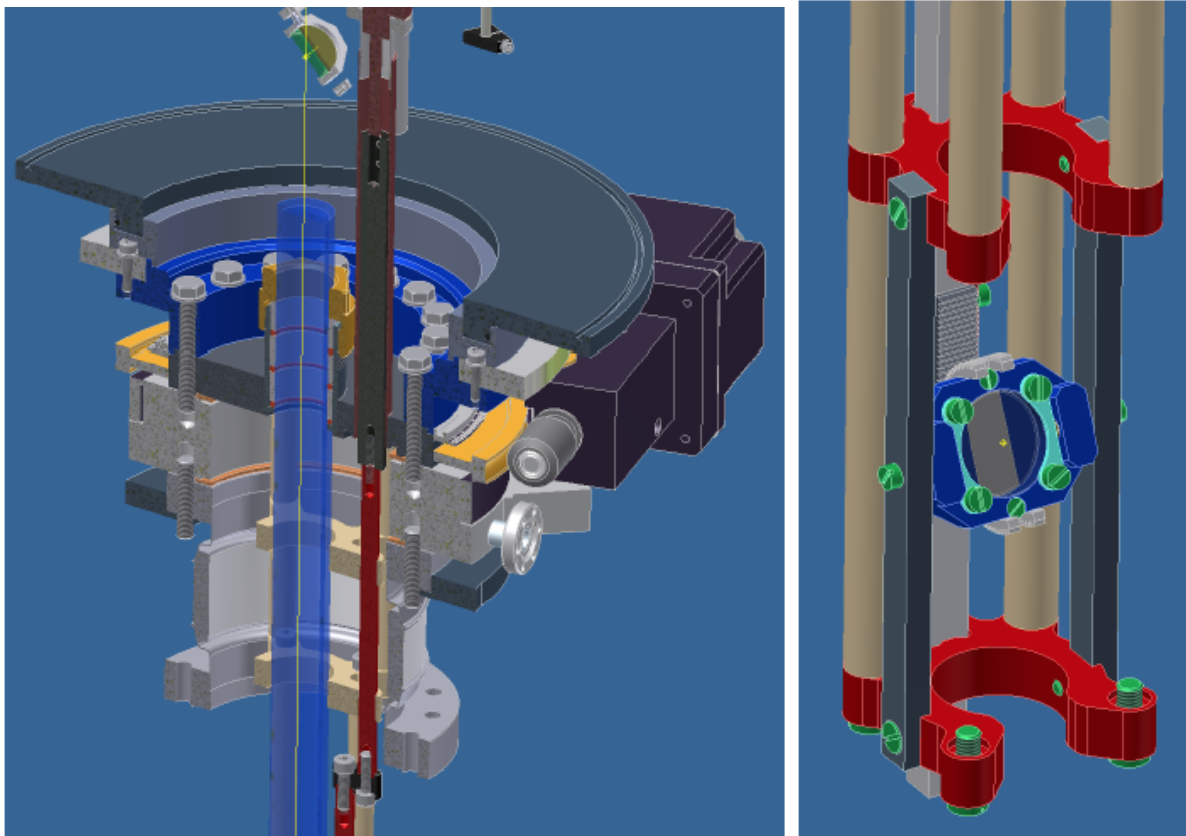


Figure 1.3: Left: CAD drawing of the MicroBooNE feedthrough. Right: CAD drawing of the MicroBooNE periscope. Both figures from[2].

313 In the case of the lasers in the end-wall ports, the beams enter the FC laterally, while in the case
 314 of the lasers in the ports over the TPC, the beams enter the TPC from the top. In both cases,
 315 the laser beam can enter the FC only through the gaps between the FC electrodes. These gaps
 316 are 1.4 cm wide and the electrodes themselves are 4.6 cm wide, so it's clear that the shadowed
 317 regions are very significant. In one of the alternative designs, the top FC is modified as to allow
 318 small openings for the bottom of the periscope to penetrate within the FC, significantly increasing
 319 coverage.

320 For the six most central ports, the distance between them is small enough that we can consider

321 having the same laser box serving two feedthroughs, in order to reduce the costs associated with
 322 the laser and its optics.

323 A scan of the full detector using 1 L volume elements would require a number of tracks on the
 324 order of 800k, would take about three days. It is expected that shorter runs could be done to
 325 investigate specific regions. The sampling granularity, and therefore the amount of data taken, is
 326 dependent on data acquisition (DAQ) requirements. In fact, even to be able to record the desired
 327 800k tracks, a dedicated data reduction algorithm will have to be devised, so that only a drift
 328 window of about $100\mu s$ of data is recorded, and the position of that window depends on the beam
 329 position and direction and which wire is being read out.

330 1.2.1.3.2 Alternative design 1: Top FC penetration

331 Given that the FC electrodes are 4.6 cm wide with only a small 1.4 cm gap between them, the
 332 shadows caused when the laser source is outside the FC are substantial. We estimate that the
 333 maximum angle at which beams can go through is about 45 deg. Given the limitations of the region
 334 above the FC, especially the geometry of the ground plane, it is likely that the mirror cannot be
 335 placed much higher up than 40 cm away from the FC. That means that, close to the top FC, the
 336 covered region will be only about 40-60 cm long, in each 3.6 m long drift volume. Considering
 337 for simplicity no limitations to movement along the direction of the FC electrodes, that means
 338 that only about 10-15% of the top area of the FC would be covered by the laser system. On the
 339 bottom FC, that ratio would be slightly higher, corresponding to the ratio of gap (1.4 cm) to total
 340 $(1.4+4.6)$ cm width, i.e. about 25%.

341 Penetration of the FC would eliminate those shadows and allow a practically unimpeded coverage.
 342 Fig. 1.4 shows a possible way to accomplish this for the top-of-TPC ports. In practice, it might
 343 be necessary to remove two FC electrodes, to achieve a 10 cm diameter free circle.

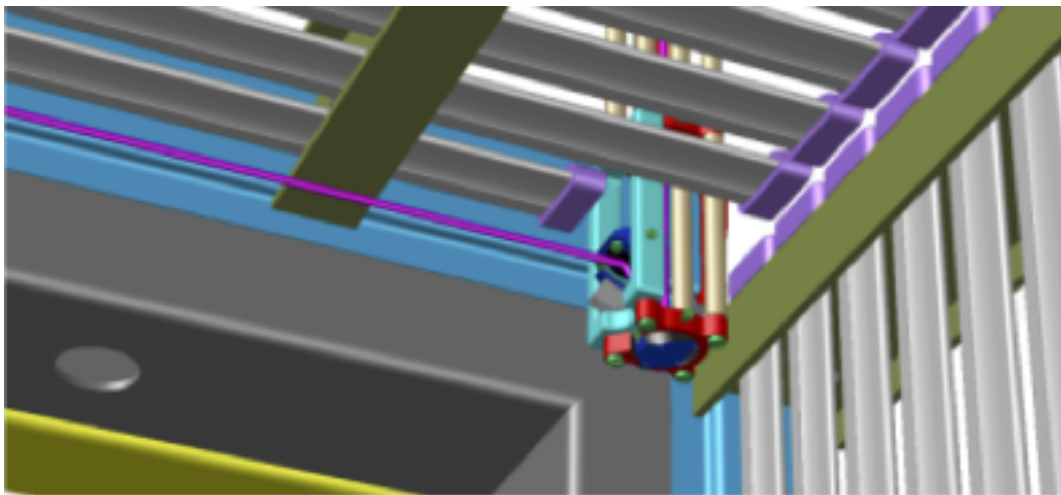


Figure 1.4: CAD drawing of a possible way for the periscope to penetrate the FC.

344 In the end-walls, such a solution is not possible since the ports are on the side, not on top of the
 345 FC. Alternative 2 addresses the coverage issues with that design.

346 1.2.1.3.3 Alternative design 2: End-wall horizontal track

347 The baseline design is based on laser entry points in which the movement of the steering mirror
348 has two angular degrees of freedom.

349 A possible alternative design would change that end part of the system so that there is a trans-
350 lation and a rotation movement. A mirror at a 45 deg angle would send the beam horizontally,
351 perpendicular to the APA/CPA, but externally to the field cage. A horizontal track, installed in
352 that same direction, would allow the translation movement of a secondary mirror (or two of them,
353 one on each side), mounted with an angle of 45 deg with respect to the incident beam. This allows
354 the mirror to be aligned with the 1.4 cm wide gaps between the field cage profiles. This second
355 mirror would have a rotation movement, around the same axis, keeping the 45 deg angle to the
356 beam, but causing its reflection to sweep a vertical plane.

357 In terms of cryostat penetration, the design of the feedthrough and periscope would follow the
358 baseline one, but the theta angle would be practical always num45 deg, with only minor adjust-
359 ments, and the angle would flip between 0 and 180 deg. The reflected beam is parallel to the
360 FC wall and perpendicular to the APA. There would have to be a new 14 m long tray for the
361 movement of the secondary mirror(s). Long plastic threaded rods could be used for the movement
362 along the tray. Rotation of the first rod would push/pull a small platform along the tray, and the
363 rotation of the second rod is transmitted to a mechanism on that platform to achieve the rotation
364 around the x axis.

365 The FC profiles are 4.6 cm wide with a 1.4 cm gap between. That's the gap close to which the
366 mirror needs to stop. That means that there is a finite amount of x values where we can position
367 the mirror, effectively every 6 cm. In order to correct for possible FC shifts, one can use the laser
368 positioning system to see if beam is passing to the other side. Choosing the z coordinate of the
369 tray to be located close to an edge of the drift volume, the the angular range of movement needed
370 to fully cover a vertical plane with the rotation of the mirror is only 90 deg.

371 The advantages of this mirror movement system are the following:

- 372 • should allow a good coverage of most of the active volume, even coming from outside the
373 FC;
- 374 • one can use the same calibration port laser to illuminate all drift volumes;
- 375 • the beam is always parallel to the APA, especially the PDS, so has less risk of hitting it
376 directly or though reflections on the cathode (but by reflections on the FC electrodes, that's
377 still possible);

378 With respect to the reference system, possible disadvantages are the following:

- 379 • in terms of construction, this option has more moving parts and movement transmitted at
380 long distances, so it can be more challenging to reach the same kind of mechanical precision
381 as the baseline one;

- if the field cage profiles shift during cooling, there will be the need to fine-tune the alignment of the mirror with the FC gaps. This could be accomplished with the laser positioning system;

1.2.1.4 Possible Measurements

The method for measurement is based on the measurement of position displacements. The laser produces straight tracks in a known position and deviations from that seen in reconstructed tracks are attributed to E field distortions. Therefore the precision with which the E field distortions can be measured depends on the precision with which we can know the laser track position and the TPC position reconstruction precision. The TPC precision is given primarily by the wire spacing of 4.7 mm in the y,z coordinates and a bit better than that (maybe 2 mm) on the z coordinate, determined by the $1\mu s$ peaking time of the electronics. Given infinite laser positioning accuracy, the smallest measurable E field distortions would be those that cause displacements of this magnitude – 2 mm in x and 5 mm in y,z. The precision on the drift velocity distortions depends on the size of the spatial region where they are present. For distortions present in regions of 0.5 m and larger, drift velocity distortions can therefore be measured with an accuracy of 1% in y,z and 0.4% in x. In y,z, 1% precision on drift velocity distortions translates to a 1% precision on the transverse field distortions. Along x, one must consider that, at 500 V/cm, a 1% change in E field leads to 0.375 % change in drift velocity. So finally, this means that the smallest measurable distortions given the TPC design (wire pitch, timing precision) are of 1% in if they are present in regions of 0.5 m and above (smaller field distortions could be in principle be measurable if they are present over larger regions, so that their effect accumulates over the drift path). On one side, this gives us an ultimate limit to the E field precision achievable with the laser system, but on the other side, since these TPC precision considerations apply to physics events too, it also tells us that an E field precision much better than 1% should not have an impact on physics.

In principle, if we were confident about the field in one detector region and would like to probe another, we could use tracks that cross both regions and use the TPC measurements in the "good" region as the "true" track direction, without needing the hardware information on the mirror angles, etc... But in a general case, the TPC precision is only one of the components of the laser measurement precision, the other being the mechanical beam positioning accuracy. The goal of the mechanical design of the system is to achieve a precision close to that of the TPC measurements, so that no single factor is dominant in the overall systematics. The starting point of the laser beams is given by the position of the mirror in the periscope, that is known from construction drawings and cool-down calculations. Warm surveys might be necessary. The angle of the beam is given the angles (theta, phi) of the mirror, that are set by the periscope motors and read-out by the encoders. Reference[13] quotes a mechanical precision of 0.05 mrad for the MicroBooNE system, for both angles. At 10 m, the maximum in MicroBooNE, that's 0.5 mm. In DUNE, we count on having 20 m long beams, so the precision is 1 mm at that distance, if we equal the precision of the MicroBooNE system. The beam itself is wider than that. In fact, with a 0.5 mrad divergence, we expect the beam to be 1 cm wide at 20 m. The profile is gaussian, so the centroid of the charge creation should be more accurate. During cool-down there can be shifts that need to be measured and corrected for, so we aim to have a system that can measure the beam position in a few positions, at least one per drift volume and laser beam. Our goal is to provide the position

424 of the beam to an accuracy of 5 mm at 15 to 20 m.

425 1.2.2 Photoelectron Laser System

426 1.2.2.1 Physics Motivation

427 Well localized electron sources represent excellent calibration tool for study of the electron trans-
428 port in the LAr TPC, identification of the inhomogeneities in the TPC electric field in all direc-
429 tions, and precise determination of the electron drift velocity. Verification and calibration of the
430 electric field distortion plays an important role in particle vertex reconstruction and identifica-
431 tion and affects the associated systematic errors, leading to increased rate of misidentification and
432 poorer energy reconstruction. Photoelectron laser can provide well localized electron sources on
433 the cathode at predetermined locations leading to improved characterization of the electric field,
434 and consequent reduction of detector instrumentation systematic error.

435 1.2.2.2 Design

436 In order to produce localized clouds of electrons using a photoelectric effect, small aluminum discs
437 or thin discs with evaporated gold film, will be used as targets. As stated in the ?? gold film can be
438 just 22 nm thick. Several photoelectric strips will compliment the circular targets to calibrate the
439 rate of transverse diffusion in LAr. Based on the experience from T2K and BNL LAr test-stand, 8-
440 10 mm diameter targets are sufficient. Targets will be placed on the cathode and distance between
441 the dots will be determined based on the calibration needs and simulations outcome. It will be
442 essential to conduct a survey of the photocathode disc locations on the cathode after installation
443 and prior to detector closing. In this way, the absolute spacial calibration of the electric field can
444 be achieved. At 266 nm NdYag quadrupled wavelength, photon energy of 4.66 eV is sufficient to
445 generate photoelectrons from both aluminum and gold. While aluminum has a lower associated
446 cost, gold film surface is easier to protect from contamination. A couple of hundred electrons are
447 expected per spill from each dot. Laser beam will be coming from the anode injection points, used
448 as sources, guided to injection points via cryogenic optical fibers with defocusing element on the
449 other end.

450 Much lower energy required for photoelectric laser, opens the possibility for a rather efficient
451 calibration of the each drift volume. Namely, laser pulse can be distributed to two drift volumes at
452 the time in order, while illuminating the entire cathode assembly. Since the photoelectron clouds
453 from different dots are very well localized, calibration of the electric field distortion in the entire
454 drift volume can be done with a single laser trigger, if the light is distributed to all injection fibers
455 for one drift volume.

456 Photoelectron laser will use the same lasers used for argon ionization. Stability of the laser pulses
457 will be monitored with powermeter. Dielectric mirrors will guide the laser light to injection points,
458 but fraction of the light will be transmitted instead of reflected to the power meter behind the

459 mirror.

460 Laser will also send forced trigger signal to the DAQ based on the photodiode that will be triggered
461 on the fraction of the light passing through the dielectric mirror. Special mirrors reflective to
462 266 nm light will be utilized.

463 1.2.2.3 Possible Measurements

464 Several measurements should be conducted to optimize the design of the photoelectron laser cal-
465 ibration system. The first thing that needs to be tested is the mounting of the targets on the
466 cathode plane assembly. In addition, survey of the dots position to the required level of precision.
467 Thickness of the target and photoelectron yield as a function of target choice, laser power and
468 attenuation of the laser light in the optical fibers.

469 1.2.3 Laser positioning system

470 1.2.3.1 Physics Motivation

471 While the direction of the laser beam will be very well known based on the reading from the
472 encoders on the laser beam steering mechanism, there will still be some residual uncertainty or
473 unpredictable shift in the pointing direction. Having in mind long length of the ionization track of
474 more than 15 m, even a small offset in the pointing direction can lead to vastly different ionization
475 track location, especially close to the end of the track. Such inaccuracies will directly impact the
476 ability to precisely calibrate any variations in the electric drift field.

477 1.2.3.2 Design

478 Laser positioning system (LPS) is designed to address the problem of precise and accurate knowl-
479 edge of the laser track coordinates. University of Hawaii group has built an LPS for the miniCAP-
480 TAIN experiment. LPS consists of groups of 9 pin diodes, operating in passive, photovoltaic mode.
481 These are GaP diodes which sensitivity range extends down to 200 nm wavelength, thus detecting
482 266 nm light is straightforward. Fig. 1.5 and Fig. 1.6 show signal detected at room and cryogenic
483 temperatures. PIN diode was illuminated by the 266 nm light from the NdYag laser (in the lab at
484 University of Hawaii) set at lowest possible setting for minimal power. Pin diode pads receive light
485 via optical fiber bundles that are mounted on the opposite side from the laser injection points to
486 eliminate issues with field cage interference. Drawings of one such group of pin diodes is shown
487 in Figs. 1.7 and Fig. 1.8. With the group of 9 photodiodes, one cannot only detect the beam but
488 also crudely characterize its profile, giving a more precise location of the central beam pulse axis.

489 There will be one LPS pad per laser. Laser would always send the first pulse in the direction of
490 the LPS before proceeding into a calibration sequence. The electronics used to collect signals from

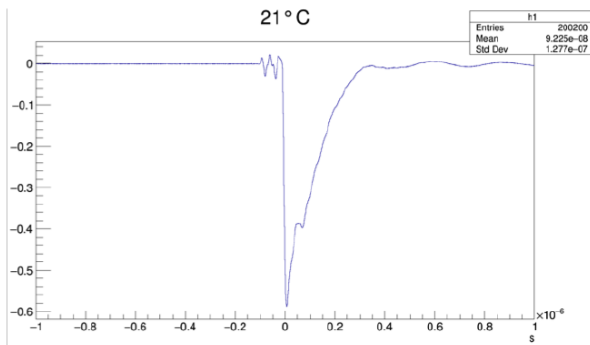


Figure 1.5: Signal from the GaP pin diode. The signal was result of illumination of the PIN diode face with 266 nm at room temperature.

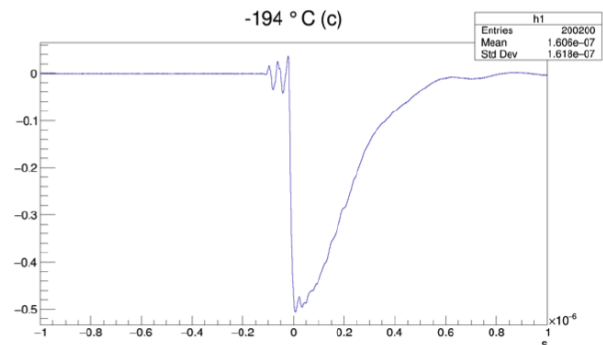


Figure 1.6: Signal from the GaP pin diode. The signal was result of illumination of the PIN diode face with 266 nm at cryogenic temperature.

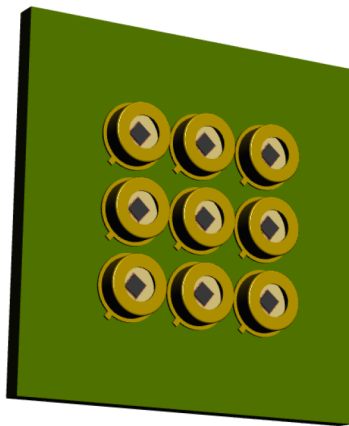


Figure 1.7: LPS cluster that is mounted on the opposite wall from the laser periscope to detect and accurately determine the end point of the laser beam.

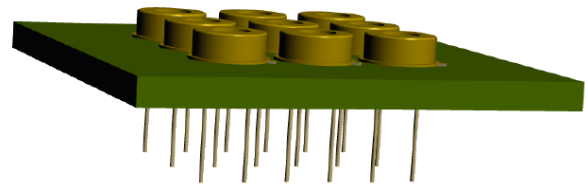


Figure 1.8: Profile of the LPS group mounted on the PCB. GaP diodes come with pins that utilize twisted pair to transport the signal.

491 the LPS will be provided by the slow control group.

492 1.2.3.3 Possible measurements

493 The utilization of the fiber bundle to deliver the 266 nm photons to LPS needs to be verified in
 494 the lab. Further optimization of the LPS assembly to reduce electronic noise and interference is
 495 required, among other things.

496 1.3 Pulsed Neutron Source Calibration System

497 1.3.1 Physics Motivation

498 In a TPC the energy reconstruction of a track depends on the amount of charge detected from
499 electrons drifting from the track to the collection plane. For a fixed amount of ionization deposited
500 at a point in the TPC, the amount of charge produced and collected depends on several factors:

- 501 1. The local electric field strength affects the fraction of charge that recombines before drifting.
502 The stronger the field, the less immediate recombination takes place, and thus the ratio of
503 drifting electrons to energy deposited increases.
- 504 2. The electron lifetime depends strongly on the purity of the argon liquid. Given the large size
505 of the DUNE TPC, the restrictions to flow in the active volume, and a likely temperature
506 gradient inside the liquid - it can be expected that there will be parts of the detector where
507 the electron lifetime will be shorter than others. The prediction of exactly how this manifests
508 is difficult to predict *ab initio*.
- 509 3. The distance electrons have to drift to be collected depends on the location of the vertex
510 inside the volume. The longer the drift, the more likely it is an electron will be absorbed.
- 511 4. Some parts of the detector can, in principle, be better or worse than others in terms of
512 noise. This can affect the threshold charge collection systematically for different areas or the
513 detector.

514 Given these facts, it is highly desirable to be able to have a "standard candle" energy deposition
515 of known energy that can be detected throughout the volume. Such a standard deposition would
516 reveal variations in the local electron collection efficiency, especially if the source could be triggered
517 such that the t_0 of the interaction was known. In principle, radioactive sources of known energy
518 distribution could be deployed throughout the detector, but there are several problems with this
519 approach: (1) the source must be physically placed at the point one wishes to check, requiring
520 multiple deployments in order to sample a significant volume of the detector, (2) the presence
521 of the source itself can alter the electric field and ionization yield, and (3) the introduction of
522 a foreign object into the active volume of the detector carries the risk of introducing impurities
523 and/or radioactive contaminants. In addition, in order to have a triggered source (and hence
524 some idea of t_0) one would have to introduce trigger electronics or other instrumentation - further
525 complicating the deployment and increasing the risk.

526 A way around this dilemma is to introduce short-lived radioactive atoms into the liquid argon
527 itself, but this has the disadvantage that there is no trigger and no way to ensure the standard
528 candle decays spread out through the whole volume. In addition, to be useful such isotopes would
529 have to have appreciable half-lives in order to have time to spread around the detector, and thus
530 the whole process might take many hours. Finally, such isotopes would likely need to be made
531 locally, which can be expensive and difficult.

532 One way around these issues is to take advantage of a remarkable property of argon - the near
533 transparency to neutrons with an energy near 57 keV due to an anti-resonance in the cross-section
534 caused by the destructive interference between two high level states of the 40-Ar nucleus. The
535 cross-section at the anti-resonance "dip" is about 10 keV wide, and at the bottom the cross section
536 of $1.6 \times 10^{-4} b$ implies an elastic scattering length of over 2,000 *m*. Thus to neutrons of this energy
537 the DUNE TPC is essentially transparent, and thus if injected from the top of the detector would
538 reach energy part of the active volume. Of course, natural argon has three major isotopes: 36-Ar
539 (0.3336%), 38-Ar (0.0834%), and 40-Ar (99.6035%) each with a slightly different anti-resonance.
540 Those that do scatter lose energy, leave the anti-resonance (where the scattering length is about
541 70 *cm*), quickly slow down and are captured. Each capture releases exactly the binding energy
542 difference between 40-Ar and 41-Ar, about 6.1 *MeV* in the form of gamma rays. As will be
543 described below, by using a *DD Generator*², a triggered pulse of neutrons can be generated outside
544 the TPC, then injected via a dedicated hole in the insulation into the liquid argon, where it spreads
545 through the entire volume to produce "standard candle" 6.1 *MeV* energy depositions. Using this
546 method, there would be no need for internal deployments, the calibration procedure would be
547 quick (likely less than 30 minutes), and there is no need to manufacture short-lived isotopes at an
548 external facility.

549 A relevant question is what fraction of neutrons slowing down from higher energy will fall into the
550 anti-resonance. Since the the average fractional energy loss of a neutron elastically scattering off
551 a 40-Argon nucleus is 4.8%, in the region of the anti-resonance the average energy loss per scatter
552 is about 3 *keV*. Therefore, estimating the width of the anti-resonance to be about 10 *keV*, a large
553 fraction of the neutrons injected can be expected to fall into the cross-section hole. Indeed, as will
554 be shown in preliminary simulations - many neutrons scatter several times before escaping to lower
555 energies to be captured. This simple phenomenon tends to scatter neutrons isotropically around
556 the liquid argon.

557 The neutron capture gamma spectrum has been measured and characterized. Recently, the ACED
558 Collaboration performed a neutron capture experiment using the Detector for Advanced Neutron
559 Capture Experiments (DANCE) at the Los Alamos Neutron Science Center (LANSCE). The result
560 was published [15] and will be used to prepare a database for the neutron capture studies.

561 1.3.2 Design

562 The basic design concept of such a pulsed neutron source has been used successfully for Boron
563 Neutron Capture Therapy[16]. The Pulsed Neutron Source will consist of three main components:
564 a DD generator, an energy moderator reducing the energy of the DD neutrons down to the desired
565 level, and the shielding materials.

566 DD generators are commercial devices that can be readily obtained from several vendors at a cost
567 of about \$ 125k each, which includes all control electronics. Pulse widths can be delivered from
568 about 10-150 μs (which affects total output). A feasible moderator has been designed using a
569 Moderator(Fe or Si)-Filter(S)- Absorber(6-Li) layered configuration. An iron moderator is used to
570 cut down the neutron energy from 2.5 MeV to below 1 MeV. Then an energy filter made of sulfur

²DD stands for "Deuterium-Deuterium"

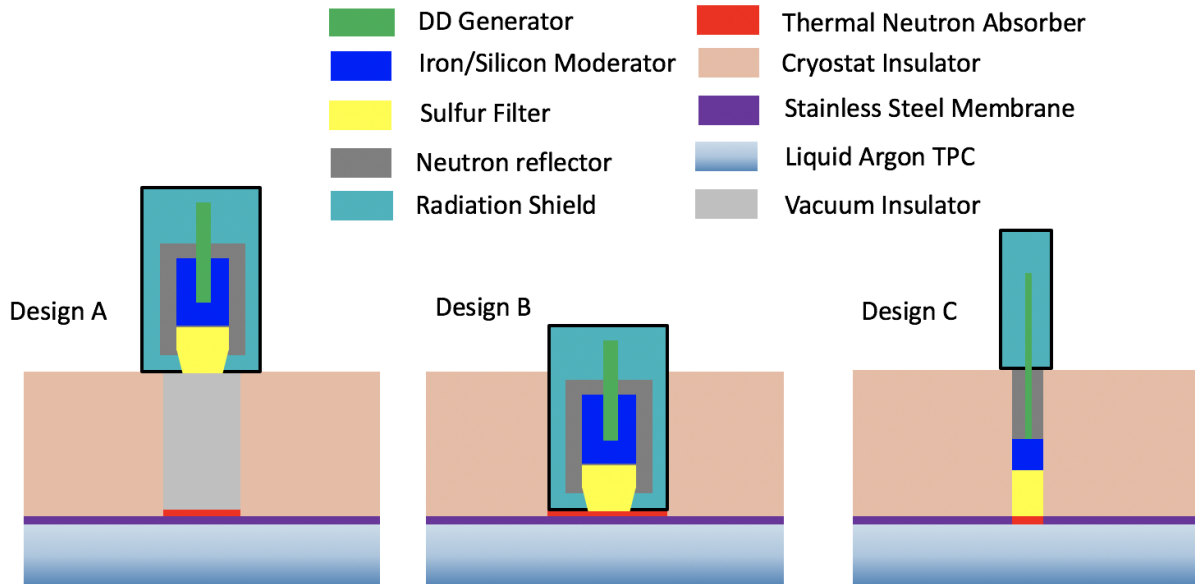


Figure 1.9: Three designs of the Pulsed Neutron Source

571 powder is used to further select the neutrons with desired anti-resonance energy. The neutron
 572 anti-resonance energy in ^{32}S is 73 keV, right above the 57 keV anti-resonance energy in ^{40}Ar .
 573 The neutrons at this energy lose about 3.0 keV per elastic scattering length. After a few elastic
 574 scattering interactions, most of the 73 keV neutrons selected by the sulfur filter will fall into
 575 the 57 keV anti-resonance energy region in liquid argon. These materials require no cooling or
 576 special handling. Finally, a thermal absorbing volume of Lithium is placed at the entry to the
 577 argon pool in order to capture any neutrons that may have fallen below the 57 keV threshold.
 578 The reflecting volume is added around the DD generator and the neutron moderator to increase
 579 downward neutron flux. The whole source will be encased in a shielding volume for safety.

580 Based on the general concept, two different designs were studied with GEANT4 simulation. Fig-
 581 ure 1.9 shows a conceptual layout of the neutron injection system.

582

583 • Design A: Large format Moderator;
 584 The neutron source is about 0.7 m wide 1 m high. It would sit above the cryostat insulator.
 585 Beneath the neutron source, a cylinder insulator volume with 50 cm diameter has to be
 586 removed to allow the neutrons to get into the cryostat. A vacuum chamber will fill the
 587 cylinder volume providing heat insulation. The cryostat stainless steel membrane will be kept
 588 closed, so no cryostat penetration is needed. The neutron source weights about 2 tons and
 589 will hang on the I-beam supporting structure. This design allows a permanent deployment
 590 of the neutron source. GEANT4 simulation has shown that 0.16 % of the neutrons generated
 591 by the DD generator are expected to be captured inside the liquid argon TPC.

592 • Design B: Large format Moderator; no insulation between Moderator and cryostat membrane
 593 The design of the the neutron source itself would be same as Design A. The only difference is
 594 that the neutron source will be placed inside a hole on the cryostat insulator. The cryostat

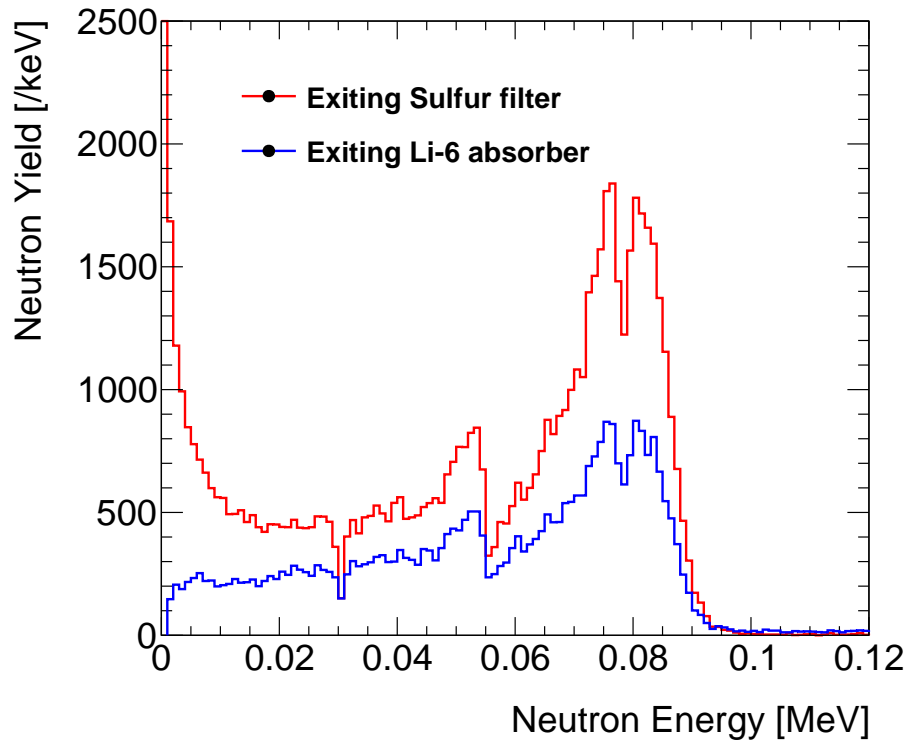


Figure 1.10: Energy of neutrons injected to the liquid argon TPC volume. Simulation based one Design B.

595 will be kept closed, but there is no vacuum insulation between the neutron moderator and
 596 the stainless steel membrane. As the neutron source is closer to the liquid argon cryostat,
 597 the neutron flux is expected to be a factor of 10 higher than that of Design A. However, the
 598 neutron source must be removed and the insulator has to be recovered after the calibration
 599 run.

- 600 • Design C: Small format Moderator; no insulation between Moderator liquid argon Design
 601 A and B require to remove a part of the cryostat insulator beneath the neutron source. If
 602 this is not available, an alternative method for delivering the neutrons is to use the existing
 603 calibration feedthroughs. In the current Cryostat design, 20 calibration feedthroughs with a
 604 20 cm diameter will be opened on top of the cryostat. One can design the neutron source
 605 with an ultra-thin DD generator that fits the size of the feedthrough. The problem is that
 606 there will be no space in the feedthrough for the shielding materials to fit in, so the neutron
 607 and gamma shield has to rely on the cryostat insulator. The weight of this compact neutron
 608 source will be about 140 kg, sufficiently low to be carried by two people. The effective
 609 neutron flux is expected to be similar as that of Design A.

610 The three designs were simulated in GEANT4. Initial simulation results indicate that two Pulsed
 611 Neutron Sources would illuminate the whole TPC volume of the DUNE far detector. Figure 1.10
 612 shows the energy spectrum of the neutrons moderated and injected to the liquid argon TPC, based
 613 on Design B. The neutron energy is moderated from 2.5 MeV to below 100 keV.

614 1.3.3 Possible Measurements

615 The path to a deployable Pulsed Neutron Source is straightforward, with measurements that
616 confirm the operation parameters, simulation results, and safety considerations. These are described
617 below.

618 1.3.3.1 Capture Cross-Section and Gamma Cascade

619 The cross-section for thermal neutron capture on argon has not been measured since the 1960's [17,
620 18, 19] and there are differences up to 40% between the central values. In addition, while the
621 integral gamma spectra has been measured via cryogenic gamma spectroscopy [?] an event-by-
622 event measurement has not yet been done. Currently, the ACED (Argon Capture Experiment
623 at DANCE) [?] is analyzing data from a November 2017 two week beam run at LANSCE that
624 will yield a cross-section measurement as a function of energy from about 0.01 eV to 1 eV (room
625 temperature thermal average is 0.0253 eV), and will also provide a library of individual capture
626 gamma cascades to put into LarSoft. It is thought that the results should be of sufficient precision
627 for use in PNS calibration design.

628 1.3.3.2 Cryostat Materials Activation Measurement

629 While DD Generators produce neutrons with relatively modest fluxes and most materials do not
630 have significant activation (which is why they are typically not used for activation studies), it is
631 prudent to have actual measurements of the activation of materials in the vicinity of the PNS to
632 be able to predict accurately the long-term activation. We propose to use the UC Berkeley DD
633 Generator facility in the Advanced Technology and Innovation Laboratory (ATIL) to expose
634 cryostat materials to many orders of DD flux (2.45 MeV) than they will see from the PNS over the
635 lifetime of DUNE. ATIL will let us use their facility for a small charge, and results will be used to
636 ensure no long-term significant activation will occur.

637 1.3.3.3 Scattering Cross-Section Measurement

638 The scattering length at the ^{40}Ar 57 keV anti-resonance has been theoretically calculated to be
639 1400 m, but since argon is 0.0629% ^{38}Ar and 0.3336% ^{36}Ar with scattering lengths of 542 m
640 and 33 m respectively, the overall scattering length of 30 m does not depend significantly on the
641 exact depth of the anti-resonance. Nevertheless, it is desirable to verify the overall scattering
642 length with a measurement at a dedicated scattering facility such as LANSCE. LANSCE has a
643 neutron Time-Of-Flight (TOF) beam with good resolution in the 10 – 100 keV range and so a
644 simple transmission experiment using a liquid argon cylindrical target of diameter 5 cm and length
645 100 – 200 cm should be more than sufficient to measure the scattering cross-section in the region
646 of interest.

647 Such an experiment will be proposed to LANSCE in March 2019 to run in early Fall 2019. Costs
648 will be minimal - with only the need to provide a LAr target with a small 2 cm thin window on
649 both ends, plus perhaps a small halo counter to reject double scatters and a collimated neutron
650 TOF detector (LANL may be able to provide this). While desirable to do, this is not critical.

651 1.3.3.4 Test Deployment in ProtoDUNE-SP

652 The post-beam run being proposed for ProtoDUNE-SP offers the opportunity to test the full
653 system (DD Generator, Moderator, Transport Model, Data Analysis) in a definitive way before
654 investing in the full PNS calibration for DUNE. The PNS group proposes to make such a run as
655 soon as resources can be identified (independent of the other measurements above), starting with a
656 commitment of engineering resources at CERN required to complete the necessary radiation safety
657 shield design, and the mechanical design necessary to support the DD Generator and Moderator.
658 The system used for ProtoDUNE-SP could also be used for ProtoDUNE-DP, and later installed
659 in the DUNE detector.

660 1.4 Alternative System: Radioactive Source Calibration Sys- 661 tem

662 1.4.1 Physics Motivation

663 Radioactive source deployment provides an in-situ source of the electrons and de-excitation prod-
664 ucts (gamma rays) which are directly relevant of physics signals from supernova neutrino and/or
665 ^8B solar neutrinos. Secondary measurements from the source deployment include electro-magnetic
666 (EM) shower characterization for long-baseline ν_e CC events, electron-lifetime as a function of
667 cryostat vertical position, and help determine radiative components of the decay electron energy
668 spectrum.

669 1.4.2 Design

670 In order to be able to observe γ -signals inside the active volume of the LArTPC from a radioactive
671 source deployed outside of the field cage, the γ -energy has be about 10 MeV. The source (for
672 safety) would be deployed about 30 cm from the field cage, so the γ -energy would need to travel
673 two attenuation lengths. Such high γ -energies are typically only achieved by thermal neutron
674 capture, which invokes a neutron source surrounded by a large amount of moderator, thus making
675 such an externally deployed (n, γ) source 20 cm to 50 cm large in diameter. In [?], a ^{58}Ni (n, γ)
676 source, triggered by an AmBe neutron source, was successfully built, yielding high γ -energies of
677 9 MeV. We propose to use a ^{252}Cf or AmLi neutron source with lower neutron energies, that requires
678 less than half of the surrounding moderator, and making the ^{58}Ni (n, γ) source only 20 cm or less

679 in diameter. The multi-purpose instrumentation feedthroughs currently planned are sufficient for
680 this, and have an inner diameter of 25 cm.

681 The activity of the radioactive source is chosen such that no more than one 9 MeV capture γ -
682 event occurs during a single 2.2 ms drift period. This allows one to use the arrival time of the
683 measured light as t_0 and then measure the average drift time of the corresponding charge signal(s).
684 The resulting drift velocity yields in turn the electric field strength, averaged over the variations
685 encountered during the drifting of the charge(s). This can be repeated for each single 9 MeV capture
686 γ -event that occurs during a 2.2 ms drift period and where visible γ -energy is deposited inside the
687 active volume of the TPC. This restricts the maximally permissible rate of 9 MeV capture γ -events
688 occurring inside the radioactive source to be less than 1 kHz, given a spill-in efficiency into the
689 active liquid argon of less than 10%.

690 A successfully employed multipurpose fish-line calibration system <insert ref> for the Double
691 Chooz reactor neutrino experiment will become available for DUNE after the decommissioning of
692 Double Chooz in 2018. The system can be easily refitted for use in DUNE. The system would be
693 deployed in four cryostat penetration multipurpose feedthroughs on the east and west ends of the
694 cryostat, which are placed at half-drift position. The sources would be deployed outside the field
695 cage within the cryostat to avoid regions with a high electric field. Also, if the source is in close
696 proximity of an APA wire frame, lower energetic radiological backgrounds become problematic as
697 the source light and charge yield is reduced exponentially with distance. The sources are removable
698 and stored outside the cryostat.

699 The commissioning plan for the source deployment system will include a dummy source deployment
700 (within 2 months of the commissioning) followed by first real source deployment (within 3-4 months
701 of the commissioning) and a second real source deployment (within 6 months of the commissioning).
702 In terms of the run plan, assuming stable detector conditions, radioactive source will be deployed
703 every half a year. Ideally, a deployment before a run period and after the run period are desired
704 so at least two data points are available for calibration and it verifies if the state of the system has
705 changed before and after the physics data run. If stability fluctuates for any reason (e.g. electronic
706 response changes over time) at a particular location, one would want to deploy the source at that
707 location once a month or more often depending on how bad the stability is. It is expected that it
708 will take a few hours (e.g. 8 hours) to deploy the system at one feedthrough location and a full
709 radioactive source calibration campaign might take at least a week.

710 1.4.3 Possible Measurements

711 Discuss development plan on way to building

712 1.5 DAQ Requirements

713 The calibration system must interface with the DUNE data acquisition system, discussed in detail
 714 in Section ???. The primary interface with calibrations will be through the DUNE Timing Sys-
 715 tem, which is responsible for providing synchronization across all subsystems and absolute time
 716 stamps, as well as for distributing triggers. Whenever possible, it is preferred that subsystems
 717 like calibrations are triggered *by* the DAQ rather than providing a trigger *to* the DAQ. Therefore
 718 the calibration systems must be designed to accept such triggers (which will have the form of a
 719 timestamp for when a trigger should occur) and it must have a way of accepting general timing
 720 information so that it is synchronized to the rest of DUNE.

721 Each calibration system will nevertheless be handled slightly differently, and each will have a
 722 different way for the DAQ to handle its data. The calibration systems could easily dominate
 723 the entire data volume for DUNE, and thus exceptions to the standard triggering and readout
 724 discussed in Section ?? are needed. We discuss below these details and the associated differences.

725 Add or reference DAQ summary table that has been prepared

726 1.5.1 Laser Calibration

727 The proposed laser source is the only practical way to unambiguously measure the electric field
 728 vectors within the detector. The field vector is determined by looking at the deflection of crossing
 729 tracks within detector voxels. The calibration group has suggested that the size of these voxels
 730 might be $10 \times 10 \times 10 \text{ cm}^3$. Because any given laser track illuminates many such voxels, one laser
 731 pulse can be used for multiple measurements—essentially the number that matters is the area of
 732 each voxel. The calibration group estimates that the number of total laser “events” would be about
 733 800,000—about half the rate of cosmic rays, and thus nominally a substantial total data volume.

Fortunately, unlike every other event type in the detector, the laser track has both a reasonably well known position and time; thus tight zero-suppression can be done for both collection and induction wires. Brett Viren suggests that a $100 \mu\text{s}$ zero suppression window is wide enough to avoid windowing problems in the induction wire deconvolution process, and we therefore assume such a window for the laser pulses. Note that the zero suppression happens *after* the trigger, not at the front-end or in the DAQ readout; thus the rate that the laser can be run will have to take into account the bandwidth through the Event Builder (where the zero-suppression would occur). From the standpoint of data volume, however, the total assuming the $100 \mu\text{s}$ zero-suppression window is:

$$800,000/\text{cal}/10 \text{ ktonne} \times 100 \mu\text{s} \times 1.5 \text{ Bytes/sample} \times 2 \text{ MHz} \times 384000 \text{ channels} = 92 \text{ TB/cal}/10 \text{ ktonne} \quad (1.1)$$

734 If such a calibration were done twice/year, then the total annual data volume for the laser is 184
 735 TB/year/10ktonne.

736 1.5.2 Radioactive Sources

737 There are two radioactive sources suggested to provide low-energy calibration data for DUNE: a
738 neutron generator source, and a γ source.

739 The neutron generator source creates a burst of neutrons which, because of the interesting neutron
740 cross section of argon, get captured throughout a large fraction of the total cryostat volume. From
741 a triggering and data volume standpoint, this is very convenient: the existing scheme of taking
742 5.4 ms of data for each trigger means all of these neutrons will be collected in a single DUNE
743 event. Thus the data volume is simply 6.22 GB times the total number of such pulses, but these
744 are likely to be few: a single burst can produce tens of thousands of neutrons whose t_0 is known
745 up to the neutron capture time of 200 μ s or so.

The γ source is somewhat more complicated to handle in the DAQ, depending on its rate. An initial proposal suggests 8 hour runs at 4 feedthroughs, and because only a single APA is being illuminated typically, the Module Level trigger could reduce the total data rate by issuing trigger commands only to the readout of the currently active APA. Nevertheless, if the rate of such a source is anywhere close to 1/5.4 ms, the detector would be running in “DC” in the current scheme. Therefore we assume that the interaction rate in the detector is 10 Hz or less. With this rate, and with localization of events to one APA, the total data volume would be

$$8 \text{ hours} \times 4 \text{ FTs} \times 10 \text{ Hz} \times 1.5 \text{ Bytes} \times 2 \text{ MHz} \times 5.4 \text{ ms} \times 2560 \text{ channels} = 50 \text{ TB/run.} \quad (1.2)$$

746 Running this calibration 4 times/year would yield 200 TB of data in 10 ktonnes per year.

747 1.5.3 Intrinsic Radioactivity

748 Mike Mooney has suggested using the intrinsic ^{39}Ar as a calibration source. This has many
749 advantages over either of the radioactive source calibrations, in particular the known level of ^{39}Ar ,
750 its uniform distribution in the detector, and the fact that it is always there and therefore integrates
751 correctly over the detector livetime. The difficulty is that because any individual ^{39}Ar event’s x
752 position is not known (because there is no t_0 , the distribution of these events must be used to
753 make measurements, thus requiring fairly high statistics.

754 Mooney’s proposal is that roughly 250,000 ^{39}Ar can provide a 1% measurement of electron lifetime.
755 (Note that 1% is a reasonable goal; if the lifetime and maximum drift time are the same, this results
756 in a 2% uncertainty on energy scale which would begin to compromise DUNE’s physics program).
757 This number of events is easily obtained with the existing random triggers as well as every other
758 trigger source excluding laser pulses and front-end calibrations.

759 Like all other parameters that must be calibrated, however, what is not clear is what the spatial and
760 temporal variations will be in the detector. Other LAr TPCs have performed lifetime calibrations
761 daily (using cosmic rays primarily), and a pixelization of 1 m² is not unreasonable, leading to a
762 need for 250,000 events for every m² in the detector each day, or about a 1 Hz trigger rate.

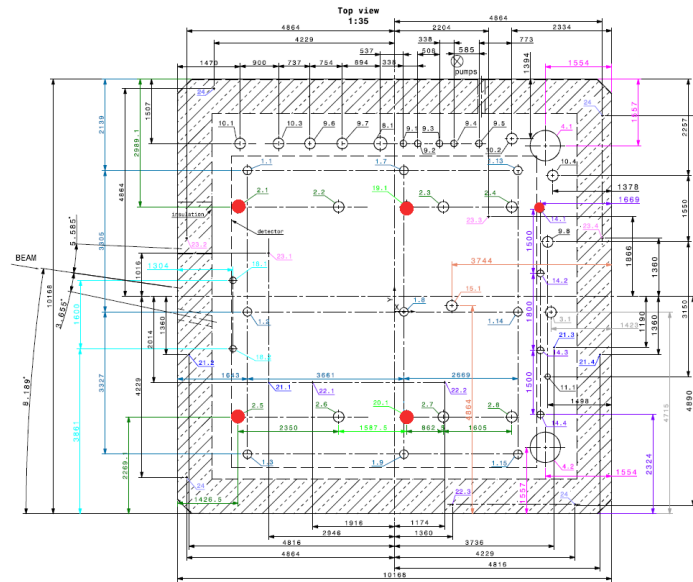


Figure 1.11: Top view of the protoDUNE-SP cryostat showing various penetrations. Ports marked in red are present free and they could be used for tests of the calibration systems. The four largest ones have the same diameter (250 mm) of the calibration ports of DUNE-FD, and are located over the TPC. The two larger ports at the right-hand side corners of the cryostat are the human access ports (or manholes).

763 In the existing scheme, this would be overwhelmingly the dominant source of data. Thus either
 764 the pixelization would need to be reduced (say, to each of the TPC volumes) or a zero-suppression
 765 scheme would have to be used. Such a zero-suppression scheme would happen post-trigger—for
 766 example, running random triggers at 1 Hz and based upon that trigger type, zero suppressing
 767 signals. In the current scheme, this would happen in the Event Builder but at 1 Hz the data rate
 768 would be too high. To do zero suppression upstream—say in the APA-level readout—based on the
 769 trigger type will likely require more hardware resources.

770 1.6 Validation of Calibration Hardware Systems

771 1.6.1 Validation in ProtoDUNE

772 All the designs presented above have aspects that warrant a validation in a situation as close as
 773 possible to the final one to be deployed in DUNE-FD. Even if there are laser calibration systems
 774 in operation in other LAr TPC experiments, the stringent requirements of such a system in terms
 775 of mechanical and optical precision, long-term reliability, track length, impact on in case of the
 776 alternative design, and DAQ interface all lead to corresponding goals of a test installation and
 777 operation in protoDUNE, that could be accomplished in the post-LS2 run. As can be seen in Fig.
 778 1.11, there are currently ports of the same size as DUNE-FD that could possibly be used for these
 779 tests. If a pair of ports are used, then one could even have crossing tracks within a single drift
 780 volume.

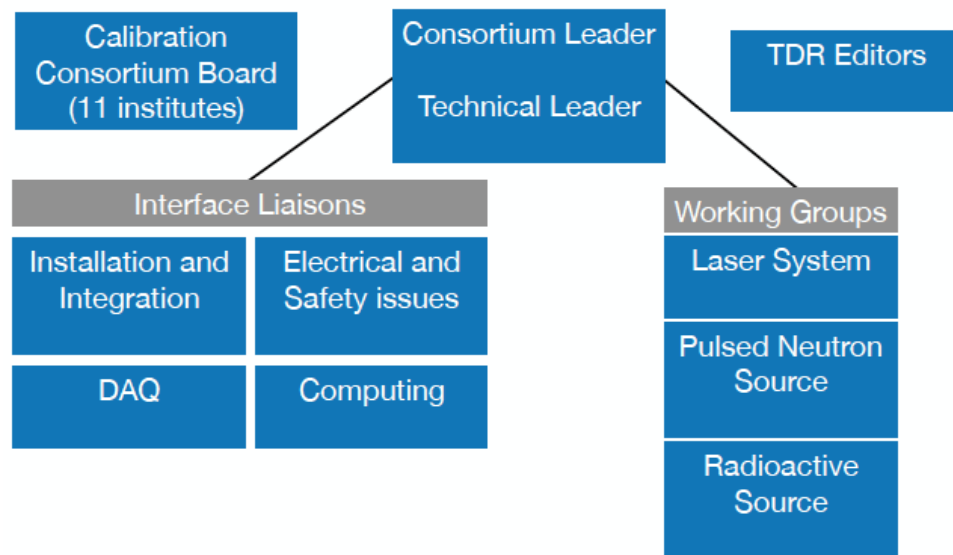


Figure 1.12: Organizational chart for the Calibration Consortium.

781 The pulsed neutron source is a new idea that has never been used in other experiments, so a
 782 protoDUNE test is especially important. The corner human access ports similar to DUNE-FD
 783 could be used for that deployment.

784 With respect to the radioactive source, the external neutron background rate is too high at surface
 785 to tests the actual gamma source. However, tests of functionality and reliability of the mechanical
 786 system are needed to demonstrate the source can be deployed and retrieved with no issues.

787 1.6.2 Validation in Other Experiments

788 1.7 Organization and Management

789 The Calibration Consortium was formed in November 2018 as a joint single and dual phase con-
 790 sortium, with a Consortium Leader and a Technical Lead.

791 Its initial mandate is the design and prototyping of a laser calibration system, a neutron generator,
 792 and a possible radioactive source system and therefore the Consortium is organized in three working
 793 groups, each dedicated to each of these systems. Each group has a designated WG leader.

794 In addition, as shown in Fig. 1.12, several liaison roles are also planned to facilitate the connection
 795 with other groups and activities:

- 796 • Detector Installation and Installation
- 797 • Electrical and Safety Issues

- 798 • DAQ
- 799 • Computing

800 There are 11 institutes in the Consortium and, as the activities progress from design to prototyping,
801 formalization of a Consortium Board is also planned.

802 1.8 Interfaces

803 Interfaces between calibration and other consortia have been identified and the appropriate docu-
804 ments are being developed. The main interfacing systems are High Voltage (HV), Photon Detection
805 System (PDS) and Data Acquisition (DAQ) and the main issues that need to be considered are
806 listed below.

807 **HV** Evaluate the effect of the calibration HW, especially the laser system periscopes, on the E field,
808 even in case of no penetration of the FC; Evaluate the effect of the incident laser beam on
809 the CPA material (kapton); Integrate the HW of the alternative photoelectron laser system
810 (targets) and the laser positioning system (diodes) within the HV system components.

811 **PDS** Evaluate long term effects of laser light, even if just diffuse or reflected, on the scintillating
812 components (TPB plates) of the PDS; Establish a laser run plan to avoid direct hits; Evaluate
813 the impact of laser light on alternative PDS ideas, such as having reflectors on the CPAs.

814 **DAQ** Evaluate DAQ constraints on the total volume of calibration data that can be acquired,
815 and develop strategies to maximize the data taking efficiency with data reduction methods;
816 Study how to implement a way to for the calibration systems to receive trigger signals from
817 DAQ, in order to maximize SN livetime.

818 1.9 Cost

819 The costs of equipment and materials and supplies for the baseline systems are described in Ta-
820 ble 1.1. To serve one SP volume, there are 20 ports for the laser; 14 ports will need one laser and
821 one feedthrough interface, but for the 6 central ports one laser will service two ports. Therefore
822 the total cost of the laser system is \$2.85M. Two pulsed neutron systems are needed for one SP
823 volume.

824 Add estimate of laser positioning system, DAQ/computers, racks? cables?

Table 1.1: Calibration System Cost Summary

System	Quantity	Cost (k\$ US)	Description
laser device	17	50.0	Laser system
feedthrough inter-face	20	100.0	Laser system; includes insulator ingress into detector and flange interface, mirrors
DD generator device	2	102.5	Pulsed Neutron Source
Moderator	2	25.1	Pulsed Neutron Source: materials to degrade neutrons to correct energy
Shielding	2	24.0	Pulsed Neutron Source: surrounding shielding
Monitor	2	16.7	Pulsed Neutron Source: Neutron monitor (device) and colimator (materials)

825 1.10 Risks

826 sample from HV - use as template

Table 1.2: High Voltage System Risk Summary

ID	Risk
(id 1)	risk text
(id 2)	risk text
...	...
(last id)	risk text

827 1.11 Quality Control

828 This is a copy of text we sent to Jim Stewart for the integration chapter.

829 The QA/QC of the calibration system parts will be done in three major steps: i) at each institute,
830 prior to shipping to ITF; ii) in ITF, prior to shipping underground; iii) a final check during/after
831 installation.

832 At ITF:

- 833 • Laser: Assembly and operation of the laser and feedthrough interface will be carried out in
834 ITF, on a mockup flange, for each of the full HW sets (periscope, feedthrough, laser, power
835 supply, electronics). All operational parts - UV laser, red alignment laser, trigger photodiode,

- 836 attenuator, diaphragm, movement motors, encoders - should be tested for functionality.
- 837 • Pulsed Neutron Source: Test operation with shielding assembled to confirm safe operating
838 conditions and sufficient neutron yields with an external dosimeter as well as with the in-
839 stalled neutron monitor. The entire system, once assembled, may be brought down the Ross
840 shaft
- 841 • Radioactive Source Deployment System: Mechanical tests including a mockup flange are done
842 at ITF. Safety checks will also be done for the source and storage above and underground.
- 843 • Radioactive Source Deployment System: Mechanical tests including a mockup flange are done
844 at ITF. Safety checks will also be done for the source and storage above and underground.
- 845 • Power supply and racks: Each of the electronics and racks will be tested prior to bringing
846 underground associated to each full system.

847 1.12 Safety

848 We consider two categories of hazards: personal risk to humans and risks of the damaging the sys-
849 tems and/or other DUNE detector components, discussed in the following subsections. These risks
850 apply in the prototyping phase, including ProtoDUNE deployment, and also during integration
851 and commissioning at the DUNE far detector site.

852 1.12.1 Human Safety

853 We also want to reference common installation and commissioning safety concerns– like work
at heights, falling object risk, overhead crane operation, heavy objects, electrical safety etc. Is
there a common document/section we can reference for this?

854 **Eye safety:** The laser system requires the operation of a class 4 laser. This requires an interlock on
855 the laser box enclosure, and only trained personnel present in the cavern for the one-time alignment
856 of the laser upon installation in the feedthroughs.

857 **Radiation:** The gammas from neutron capture on hydrogen could bring a potential radiation
858 safety concern for the PNS. The design of key safety systems (custom shielding and moderator)
859 for the PNS will be discussed with safety experts at CERN and at MSU prior to operation at
860 ProtoDUNE. In particular, the entire system will be assembled in a neutron shielded room and
861 tested to confirm there is no leak of neutrons. The system will also have a neutron monitor which
862 can be used to provide an interlock.

863 The RS also poses a radiation risk, which will be mitigated with a glovebox for handling, and a

864 shielded storage box and area.

865 1.12.2 Detector and System Safety

866 We consider risks to the calibration systems themselves, and also to other DUNE materials or
867 systems.

868 This may be a shared concern. We want to avoid bumping/breaking components as they are checked, installed and commissioned in DUNE. Special care will need to be taken to install components and do checks stepwise.

869 **Mechanical damage:** The deployed radioactive source can potentially swing into detector elements
870 if not controlled or if large currents exist in the liquid argone. Guidewires mitigate this risk.

871 **Laser system protection:** If the too much water enters the laser system port, then ice may block
872 the laser.

873 Jose, mitigation is?

874 **Damage to the photon detection system by the laser:** To mitigate possible damage to the
875 PD system, software will be used to block the beam while the mirrors are stopped or when laser
876 light is directed at the PD system. Initial discussion with PDS indicates that this may not be a
877 significant issue.

878 relationship between this and interface with PD?

879 **Radiation damage to DUNE components:** The activation caused by the PNS is being studied
880 and will be known by ProtoDUNE testing for the PNS at neutron flux intensities and durations
881 well above the run plan.

882 May also need to reference background TF. Add RS system.

883 We have started discussions about electrical safety and grounding, and will update this once formal documents are prepared for that.

884 1.13 Installation, Integration and Commissioning

885 This is a copy of text we sent to Jim Stewart for the integration chapter. We need guidance for how this chapter and that chapter need to reference each other.

886 **1.13.1 ITF integration**

887 The laser positioning system has to be integrated with the HV system in the ITF before shipping
888 underground (underground). Two components (baseline design: mirror clusters, and alternative
889 design: diodes) would require interface with the HV and field cage structural systems, discussed
890 below.

891 The baseline consists of a set of about 40 mirror clusters - a plastic piece holding 4 to 6 small
892 mirrors (5 mm diameter), each at a different angle - to which the ionization laser will point in order
893 to obtain an absolute pointing reference. These clusters will be attached to the bottom field cage
894 cross bars facing into the TPC. These cross bars must contain small alignment slots, matching the
895 cluster pieces, in order for us to know the exact position of each cluster. This attachment/assembly
896 of the mirror clusters on corresponding the FC cross-bars must be done in the ITF before shipping
897 the HV system underground.

898 An alternative design, that can be done in addition to the mirror clusters, which, following on
899 the mini-CAPTAIN experience, is based on a set of diodes that fire when the laser beam hits
900 them. Since the laser shoots from above, and the diodes need to be in a low voltage region, the
901 plan is to attach them to the bottom ground plane, facing into the bottom FC. For the pointing
902 measurement, the beams will pass through the FC electrodes and hit the diodes below. At least
903 20 of these diode clusters would be installed, and this assembly on the ground planes needs to be
904 done in the ITF as well.

905 **1.13.2 Installation**

906 Only the laser system alternative design has components that need to be installed inside the cryostat
907 via the TCO. The pulsed neutron source and radioactive source deployment systems are installed
908 only using the cryostat roof ports.

909 Laser, inside TCO: A long horizontal track system is to be installed outside the end-wall field
910 cage, directly below the corresponding calibration ports, and suspended by them. The system
911 farthest away from the TCO must be installed before TPC (FC/APA/CPA) installation begins.
912 This installation requires the simultaneous installation of the corresponding periscopes, from the
913 calibration ports, so that the two systems can be properly connected. The relevant QC is essentially
914 alignment test.

915 In addition, the alternative laser positioning system has sets of photo-diodes pre-mounted on
916 the HV system bottom ground planes. The only step that needs to be done inside the TCO is
917 connecting the cabling to available flange (still working out how to route cables and which flange
918 to use).

919 Laser, outside TCO: The periscopes on the top of the TPC in the center can be installed after
920 the relevant structural elements (e.g. field cage), these proceed in sequence with the assembly of
921 other components (furthest from TCO is assembled first) and alignments can be done as elements

922 are installed with the alignment laser system. Once for each periscope/laser system, prior to the
 923 installation of further TPC components, we will need to clear the cavern to align the UV (Class
 924 4) and visible lasers this will need special safety precautions. It may be possible to do this special
 925 alignment operation for all lasers at roughly the same time, to minimize the disruption.

926 A support beam structure closest to the TCO temporarily blocks the calibration ports, this is
 927 removed after the last TPC component. After that, the final calibration components can be
 928 installed, including the the periscopes on the TCO endwall and the horizontal track closest to the
 929 TCO would be the last items to be installed.

930 Pulsed Neutron Source: The pulsed neutron source will be installed after the human access ports
 931 are closed as it sits above them. Final QC will be operating the source and measuring the flux
 932 with integrated monitor and dosimeter.

933 Power supply and racks: Space on mezzanine close to each calibration port is important in order
 934 to power and operate the calibration systems (laser and PNS). They can be installed following the
 935 associated periscope installation.

936 Radioactive Source Deployment System: The RSDS guide system can be installed as the first
 937 element before TPC elements for the endwall furthest from the TCO, and the last system (con-
 938 current and coordinated with the alternative laser system). The RSDS is installed at the top of
 939 the cryostat and can be installed when DUNE is working.

940 1.14 Institutional Responsibilities

941 Currently, the calibration consortium has the following member institutions: University of Bern
 942 (Bern), Boston University (BU), Colorado State University (CSU), University of California, Davis
 943 (UC Davis) University of Hawaii (Hawaii), University of Iowa (Iowa), LIP, Michigan State Univer-
 944 sity (MSU), University of Pittsburgh (Pitt), South Dakota School of Mine Technology (SDSMT),
 945 and University of Tennessee, Knoxville (UTK). The responsibilities of each group are described in
 946 Table 1.3.

947 Need to confirm this with groups, esp CSU, Pitt doing general simulation work and under-
 stand what further subdivision is useful. We are also seeking new groups.

Table 1.3: Institutional responsibilities in the Calibration Consortium

System	Institutional Responsibility
Laser System	Bern, Hawaii, LIP, Pitt, UTK
Pulsed Neutron Source	BU, CSU, UC Davis, Iowa, LIP, MSU, SDSMT

948 1.15 Schedule and Milestones

949 Table 1.4 shows the milestones for the Pulsed Neutron System.

950 The laser system schedule will look similar to the pulsed neutron source– but we need to confirm the TCO closing/installation period before filling in a table for it.

Table 1.4: Pulsed Neutron Source Schedule

Milestone	Date (Month YYYY)
Design optimization process: beam width, moderator, shielding and cryostat interface	Mar 2020
Perform neutron moderator test and cryostat material activation test	Mar 2020
Complete instrument safety and neutron yield test. Confirm remote operation.	Mar 2021
Demonstration test at ProtoDUNE	Aug 2022
Assembly of additional device	Mar 2023
Installation and commissioning	Jun 2023

Glossary

- 951
- 952 **anode plane assembly (APA)** A unit of the SP detector module containing the elements sensitive
953 to ionization in the LAr. It contains two faces each of three planes of wires, and interfaces
954 to the cold electronics and photon detection system. 4
- 955 **cold electronics (CE)** Refers to readout electronics that operate at cryogenic temperatures. 1
- 956 **data acquisition (DAQ)** The data acquisition system accepts data from the detector FE electron-
957 ics, buffers the data, performs a trigger decision, builds events from the selected data and
958 delivers the result to the offline secondary DAQ buffer. 9
- 959 **detector module** The entire DUNE far detector is segmented into four modules, each with a
960 nominal 10 kt fiducial mass. 6, 34
- 961 **secondary DAQ buffer** A secondary DAQ buffer holds a small subset of the full rate as selected
962 by a trigger command. This buffer also marks the interface with the DUNE Offline. 33
- 963 **DP module** dual-phase detector module. 4
- 964 **detector support system (DSS)** The system used to support the SP detector within the cryostat.
965 iii, 3
- 966 **field cage (FC)** The component of a LArTPC that contains and shapes the applied E field. 3
- 967 **far detector (FD)** Refers to the 40 kt fiducial mass DUNE detector to be installed at the far site
968 at SURF in Lead, SD, to be composed of four 10 kt modules. 4
- 969 **high voltage (HV)** Generally describes a voltage applied to drive the motion of free electrons
970 through some media. 1, 4
- 971 **liquid argon (LAr)** The liquid phase of argon. 6, 8, 24
- 972 **long-baseline (LBL)** Refers to the distance between the neutrino source and the far detector. It
973 can also refer to the distance between the near and far detectors. The “long” designation is
974 an approximate and relative distinction. For DUNE, this distance (between Fermilab and
975 SURF) is approximately 1300 km. 1

- 976 **MicroBooNE** The LArTPC-based MicroBooNE neutrino oscillation experiment at Fermilab. iii,
977 6, 8, 11
- 978 **photon detection system (PDS)** The detector subsystem sensitive to light produced in the LAr.
979 1
- 980 **trigger candidate** Summary information derived from the full data stream and representing a
981 contribution toward forming a trigger decision. 34
- 982 **trigger command** Information derived from one or more trigger candidates that directs elements
983 of the detector module to read out a portion of the data stream. 33, 34
- 984 **trigger decision** The process by which trigger candidates are converted into trigger commands.
985 33, 34

References

- 987 [1] The ICARUS-WA104, LAr1-ND and MicroBooNE Collaborations, “A Proposal for a Three
988 Detector Short-Baseline Neutrino Oscillation Program in the Fermilab Booster Neutrino
989 Beam,” tech. rep., 2015. <https://arxiv.org/abs/1503.01520>.
- 990 [2] R. Acciarri *et al.*, “Design and construction of the microboone detector,” *Journal of*
991 *Instrumentation* **12** no. 02, (2017) P02017.
992 <http://stacks.iop.org/1748-0221/12/i=02/a=P02017>.
- 993 [3] DOE Office of High Energy Physics, “Mission Need Statement for a Long-Baseline Neutrino
994 Experiment (LBNE),” tech. rep., DOE, 2009. LBNE-doc-6259.
- 995 [4] M. Mooney, “Space charge effects in lartpcs,” *Workshop on Calibration and Reconstruction*
996 *for LArTPC Detectors* (2018) . [https://indico.fnal.gov/event/18523/session/19/](https://indico.fnal.gov/event/18523/session/19/contribution/29/material/slides/0.pdf)
997 [contribution/29/material/slides/0.pdf](https://indico.fnal.gov/event/18523/session/19/contribution/29/material/slides/0.pdf).
- 998 [5] The DUNE Collaboration, “The DUNE Far Detector Interim Design Report Volume 1:
999 Physics, Technology Strategies,” tech. rep., 2018. <https://arxiv.org/abs/1807.10334>.
- 1000 [6] The DUNE Collaboration, “The DUNE Far Detector Interim Design Report Volume 2:
1001 Single-Phase Module,” tech. rep., 2018. <https://arxiv.org/abs/1807.10327>.
- 1002 [7] W. Walkowiak, “Drift velocity of free electrons in liquid argon,” *Nuclear Instruments and*
1003 *Methods in Physics Research Section A: Accelerators, Spectrometers, Detectors and*
1004 *Associated Equipment* **449** (2000) 288 – 294.
- 1005 [8] B. Rossi *et al.*, “A prototype liquid argon time projection chamber for the study of uv laser
1006 multi-photonic ionization,” *Journal of Instrumentation* **4** (2009) P07011.
1007 <https://arxiv.org/abs/0906.3437>.
- 1008 [9] M. Zeller *et al.*, “First measurements with ARGONTUBE, a 5m long drift Liquid Argon
1009 TPC,” *Nucl. Instrum. Meth.* **A718** (2013) 454–458.
- 1010 [10] A. Ereditato *et al.*, “A steerable uv laser system for the calibration of liquid argon time
1011 projection chambers,” *Journal of Instrumentation* **9** (2014) T11007.
1012 <https://arxiv.org/abs/1406.6400>.

- 1013 [11] A. Ereditato, D. Goeldi, S. Janos, I. Kreslo, M. Luethi, C. Rudolf von Rohr, M. Schenk,
1014 T. Strauss, M. S. Weber, and M. Zeller, “Measurement of the drift field in the
1015 ARGONTUBE LAr TPC with 266 nm pulsed laser beams,” *JINST* **9** no. 11, (2014) P11010,
1016 arXiv:1408.6635 [physics.ins-det].
- 1017 [12] The CAPTAIN Collaboration, “The CAPTAIN Detector and Physics Program,” tech. rep.,
1018 2013. <https://arxiv.org/abs/11309.1740>.
- 1019 [13] Y. Chen, “Laser calibration at lar tpcs,” *Workshop on Calibration and Reconstruction for*
1020 *LArTPC Detectors* (2018) . [https://indico.fnal.gov/event/18523/session/17/](https://indico.fnal.gov/event/18523/session/17/contribution/35/material/slides/0.pdf)
1021 [contribution/35/material/slides/0.pdf](https://indico.fnal.gov/event/18523/session/17/contribution/35/material/slides/0.pdf).
- 1022 [14] I. Badhrees *et al.*, “Measurement of the two-photon absorption cross-section of liquid argon
1023 with a time projection chamber,” *New Journal of Physics* **12** (2010) 113024.
1024 <https://iopscience.iop.org/article/10.1088/1367-2630/12/11/113024>.
- 1025 [15] V. Fischer *et al.*, “Measurement of the neutron capture cross-section on argon,”
1026 arXiv:1902.00596 [nucl-ex] .
- 1027 [16] H. Koivunoro, D. Bleuel, U. Nastasi, T. Lou, J. Reijonen, and K.-N. Leung, “Bnct dose
1028 distribution in liver with epithermal d-d and d-t fusion-based neutron beams,” *Applied*
1029 *Radiation and Isotopes* **61** no. 5, (2004) 853 – 859.
1030 <http://www.sciencedirect.com/science/article/pii/S0969804304003409>. Topics in
1031 Neutron Capture Therapy: Proceedings of the Eleventh World Congress on Neutron
1032 Capture Therapy (ISNCT-11).
- 1033 [17] W. Koehler, “The activation cross section of ^{40}Ar for thermal neutrons,” *Zeitschrift fuer*
1034 *Naturforschung (West Germany) Divided into Z. Naturforsch., A, and Z. Naturforsch., B:*
1035 *Anorg. Chem., Org. Chem., Biochem., Biophys.*, **18a** (12, 1963) .
- 1036 [18] R. French and B. Bradley, “The ^{40}Ar thermal activation cross-section and resonance
1037 integral,” *Nuclear Physics* **65** no. 2, (1965) 225 – 235.
1038 <http://www.sciencedirect.com/science/article/pii/0029558265902658>.
- 1039 [19] N. Ranakumar, E. Karttunen, and R. Fink, “Thermal and 14.4 MeV neutron activation cross
1040 sections of argon,” *Nuclear Physics A* **128** no. 1, (1969) 333 – 338.
1041 <http://www.sciencedirect.com/science/article/pii/0375947469909968>.